# $Yb_{14}MnSb_{11}$: New High Efficiency Thermoelectric Material for Power Generation

Shawna R. Brown,[†] Susan M. Kauzlarich,*[,†] Franck Gascoin,[‡] and G. Jeffrey Snyder*[,‡]

*Department of Chemistry, University of California, One Shields Avenue, Davis, California 95616, and Jet Propulsion Laboratory, California Institute of Technology, 4800 Oak Grove Drive, Pasadena, California 91109-8099*

*Received February 2, 2006*

Thermoelectric materials provide a key solution to energy problems through the conversion of heat into electrical energy. We report that the complex Zintl compound, $Yb_{14}MnSb_{11}$, breaks a 2-decade stagnation in high-temperature (>900 K), p-type materials development for thermoelectric power generation. This material achieves quadrupled efficiency and virtually doubled figure of merit over the current state-of-the-art, SiGe, thus earmarking it superior for thermoelectric applications in segmented devices. $Yb_{14}MnSb_{11}$ represents the first complex Zintl phase with substantially higher figure of merit and efficiency than any other competing materials, opening a new class of thermoelectric compounds with remarkable chemical and physical properties.

## Introduction

The study of thermoelectrics has seen renewed interest in the past decade, spurred not only by increasing environmental and energy conservation issues, such as the necessity for the elimination of chlorofluorocarbons and the utilization of waste heat in automobiles, but also by the need for improved power sources for deep space probes. Improved efficiency for applications such as spacecraft power requires thermoelectric materials that can operate at high temperatures (above 975 K) and can be effectively incorporated into segmented thermoelectric converters.[1] Several complex structure types[2−11] with recently discovered unexpected and exceptional thermoelectric properties have revived interest in the search for more efficient thermoelectric materials; however, the high-temperature p-type region has lagged in materials development, thus limiting attainable device efficiency. In fact, the state-of-the-art material, SiGe, has remained the most commonly used material for over 2 decades.[12] Breakthrough figures of merit have been regularly achieved in n-type materials operative from 300 to 1272 K and p-materials operative at lower temperatures (300−975 K); however, the high-temperature p-region has not seen such an advance until now.

Interest in $Yb_{14}MnSb_{11}$ (Figure 1) as a high-performance, high-temperature thermoelectric was initiated because of its exceptional electronic properties,[13−17] its complex structure consisting of a variety of distinct structural units, and its potential to be optimized because of the large array of elements found in this structure type. This report presents a figure of merit (zT) that has never been achieved in the high-temperature p-type region, a 4-fold advancement of conversion efficiency for segmented thermoelectric materials and improved compatibility (*s*). It also introduces a chemically rich, bulk material that can be further optimized for higher efficiency segmented thermoelectric devices. Until now, p-$Si_{1-x}Ge_x$ alloy (SiGe), with $x \sim 0.3$, has been the superior high-temperature material with a maximum $zT \sim 0.6$;[12,18] $Yb_{14}MnSb_{11}$ improves this figure of merit by at least 67%.

To determine the thermoelectric efficiency of a segmented thermoelectric device, there are two primary parameters that govern performance, the thermoelectric figure of merit (zT) and the temperature difference ($\Delta T$) across the module ($zT = \alpha^2 T/\rho\kappa_T$ where $\alpha$ is the Seebeck coefficient ($\mu$V/K), $T$ is temperature (K), $\rho$ is electrical resistivity (m$\Omega$-cm), and

* To whom correspondence should be addressed. E-mail: smkauzlarich@ucdavis.edu; jsnyder@jpl.nasa.gov.
† University of California.
‡ California Institute of Technology.

(1) Snyder, G. J. *Appl. Phys. Lett.* **2004**, *84* (13), 2436−2438.
(2) Okamoto, N. L.; Nishii, T.; Oh, M. W.; Inui, H. *Mater. Res. Soc. Symp. Proc.* **2004**, *793* (Thermoelectric Materials 2003--Research and Applications), 187−192.
(3) Sales, B. C.; Mandrus, D.; Williams, R. K. *Science (Washington, D. C.)* **1996**, *272* (5266), 1325−1328.
(4) Kim, S. W.; Kimura, Y.; Mishima, Y. *Sci. Technol. Adv. Mater.* **2004**, *5* (4), 485−489.
(5) Bilc, D.; Mahanti, S. D.; Quarez, E.; Hsu, K.-F.; Pcionek, R.; Kanatzidis, M. G. *Phys. Rev. Lett.* **2004**, *93* (14), 146403/1−146403/4.
(6) Venkatasubramanian, R.; Siivola, E.; Colpitts, T.; O'Quinn, B. *Nature* **2001,** *413* (Oct 11) (6856), 597−602.
(7) Harman, T. C.; Spears, D. L.; Manfra, M. J. *J. Electron. Mater.* **1996**, *25* (7), 1121−1127.
(8) Beyer, H.; Nurnus, J.; Bottner, H.; Lambrecht, A.; Roch, T.; Bauer, G. *Appl. Phys. Lett.* **2002**, *80* (7), 1216−1218.
(9) Yamanaka, S.; Kosuga, A.; Kurosaki, K. *J. Alloys Compd.* **2003**, *352* (1−2), 275−278.
(10) Kurosaki, K.; Kosuga, A.; Muta, H.; Uno, M.; Yamanaka, S. *Appl. Phys. Lett.* **2005**, *87* (6), 061919/1−061919/3.
(11) Wolfing, B.; Kloc, C.; Teubner, J.; Bucher, E. *Phys. Rev. Lett.* **2001**, *86* (19), 4350−4353.
(12) Wood, C. *Energy Conversion Manage.* **1984**, *24* (4), 331−343.
(13) Fisher, I. R.; Wiener, T. A.; Bud'ko, S. L.; Canfield, P. C.; Chan, J. Y.; Kauzlarich, S. M. *Phys. Rev. B: Condens. Matter Mater. Phys.* **1999**, *59* (21), 13829−13834.
(14) Fisher, I. R.; Bud'ko, S. L.; Song, C.; Canfield, P. C.; Ozawa, T. C.; Kauzlarich, S. M. *Phys. Rev. Lett.* **2000**, *85* (5), 1120−1123.
(15) Chan, J. Y.; Olmstead, M. M.; Kauzlarich, S. M.; Webb, D. J. *Chem. Mater.* **1998**, *10* (11), 3583−3588.
(16) Holm, A. P.; Ozawa, T. C.; Kauzlarich, S. M.; Morton, S. A.; Waddill, G. D.; Tobin, J. G. *J. Solid State Chem.* **2005**, *178* (1), 262−269.
(17) Holm, A. P.; Kauzlarich, S. M.; Morton, S. A.; Waddill, G. D.; Pickett, W. E.; Tobin, J. G. *J. Am. Chem. Soc.* **2002**, *124* (33), 9894−9898.
(18) Yamashita, O.; Sadatomi, N. *J. Appl. Phys.* **2000**, *88* (1), 245−251.

10.1021/cm060261t CCC: $33.50 
Published on Web 03/09/2006

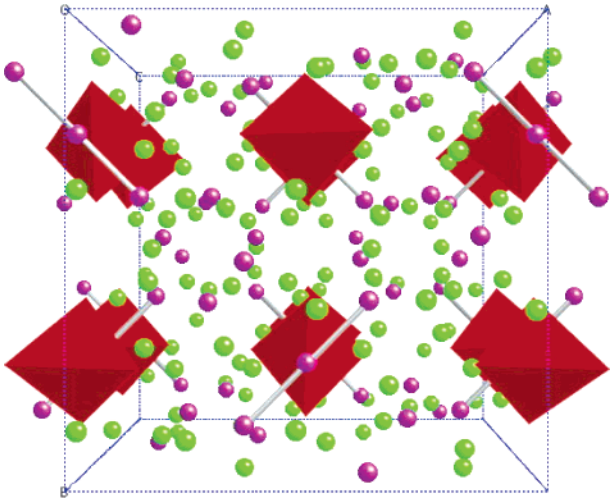

**Figure 1.** Body-centered, $I4_1/acd$ crystal structure of $Yb_{14}MnSb_{11}$. The green and purple spheres represent Yb and Sb, respectively. The $MnSb_4$ tetrahedron is shown as a filled red polyhedron.

$\kappa_T$ is thermal conductivity (mW/cm·K);[19] $\Delta T = T_h - T_c$ where $T_h$ is the hot side of the device and $T_c$ is the cold side of the device). The temperature difference between $T_h$ and $T_c$ sets the upper limits of efficiency through the Carnot efficiency, $\eta_c = \Delta T/T_h$.[1] The materials segmented in the device determine how close the efficiency will be to the Carnot maximum through zT. It is important to note that the efficiency of a thermoelectric generator depends on the Carnot factor and the reduced efficiency which is a function of zT. Therefore, for high efficiency, a large zT is required throughout a large temperature range. Often, the electrical properties of a material are examined through the thermoelectric power factor, $P = \alpha^2/\rho$.[20]

When materials are being segmented for high-efficiency, large temperature gradient applications, thermoelectric compatibility factors ($s = [(1 + zT)^{1/2} - 1]/\alpha T$) must be considered because to maintain maximum efficiency the same electrical current and similar heat must flow through each segment.[1] If the compatibility factors differ (by more than about a factor of 2) not all the segments will perform with the utmost effectiveness, such that the overall efficiency will be substantially less than that predicted from the individual material's average zT. This is particularly a problem for high-temperature p-type segments where the state-of-the-art high-temperature material, SiGe, has a much lower compatibility factor than other good p-type materials, making it incompatible for segmentation.

Good thermoelectric compounds have low electrical resistivity, low thermal conductivity, and a large Seebeck coefficient.[19] Typically, small band-gap, semiconducting materials with carrier concentrations within $10^{19}$−$10^{21}$ $cm^{-3}$ work better than metals or insulators.[21] Also, a large unit cell, heavy atoms, and structural complexity generally result in good thermoelectric efficiency. Many Zintl materials fulfill these qualifications; however, relatively few have been investigated.[22]

Materials included in the Zintl class are, in general, electronically positioned between intermetallics and insulating compounds.[23] These materials are considered to be valence precise[24] and form the requisite small band gap semiconductors with complex structures. Often they contain cationic sites that allow for the addition of disordered scattering and the tuning of carrier concentration (and therefore the electronic properties).[22]

$Yb_{14}MnSb_{11}$, even though considered to be a Zintl, stretches the boundaries of the classical model. This material is isostructural to the Zintl phase, $Ca_{14}AlSb_{11}$, and maintains valence precision (holding true to the Zintl definition). Each formula unit of this structure type consists of one $[AlSb_4]^{9-}$ tetrahedron, a $[Sb_3]^{7-}$ polyatomic anion, four $Sb^{3-}$ anions, and 14 $Ca^{2+}$ where in the Zintl extreme these units would be considered as being held together through ionic forces.[25]

$Yb_{14}MnSb_{11}$ however, is not a typical semiconductor: X-ray photoelectric spectroscopy (XPS)[16] shows a weakly metallic or semimetallic Fermi edge while resistivity measurements below room temperature are indicative of a metal.[15] Clearly, the bonding in $Yb_{14}MnSb_{11}$ is more complex than that in $Ca_{14}AlSb_{11}$. X-ray magnetic circular dichroism (XMCD)[17] and XPS[16] measurements show that, indeed, the ytterbium is in the $Yb^{2+}$ valence state, replacing $Ca^{2+}$; however, the manganese has been shown to be in the $Mn^{2+}$ valence state, supplying one less electron than $Al^{3+}$. This shortage of electrons ($1.3 \times 10^{21}$ holes/$cm^3$) explains the material's p-type behavior and corresponds well to the measured carrier concentration by Hall effect (below).

The generic expression for this structure type is $A_{14}MPn_{11}$, where A is a heavy or alkaline earth metal, M is a transition or main group metal, and Pn is a pnicogen. The various sites allow for the potential tuning of the electronic and thermal properties through doping. Doping on the cationic metal site, A, allows for possible tuning of the carrier concentration and disorder scattering of phonons, while doping on the metal site, M, enables possible tuning of the electronic parameters.

## Experimental Section

**Single-Crystal Synthesis.** All materials were handled in a nitrogen-filled drybox with water levels below 1.0 ppm. Sublimed dendritic Yb metal (Alfa Aesar, 99.99%) was cut into small pieces and used as received. Mn chips (Alfa Aesar, 99.98%) were ground into a powder. Sb chunks (Allied Chemical, 99.7%) and Sn granules (Mallinckrodt, 99.967%) were used as received. $Yb_{14}MnSb_{11}$ was synthesized via a Sn flux.[13,16,26] The elements, Yb:Mn:Sb:Sn, were arranged in 2 $cm^3$ and 5 $cm^3$ $Al_2O_3$ crucibles in the ratios 14:6:11:86. The reactions were sealed in quartz ampules under 1/5 atm argon atmosphere and placed in high-temperature programmable furnaces. The reactions were brought up to 1100 °C following the heating procedure by Fisher et al.[13] Once at 1100 °C the reactions were held for 1 h and then cooled to temperatures between 700 and 800 °C at a rate of 2−3 °C/h. Upon reaching final temperatures,

(19) DiSalvo, F. J. *Science (Washington, D. C.)* **1999**, *285*, 703−706.
(20) Goldsmid, H. J.; Nolas, G. S. *Int. Conf. Thermoelectr.* **2001**, *20*, 1−6.
(21) Mahan, G.; Sales, B.; Sharp, J. *Phys. Today* **1997**, *50* (3), 42−47.
(22) Gascoin, F.; Ottensmann, S.; Stark, D.; Haile, S. M.; Snyder, G. J. *Adv. Funct. Mater.* **2005**, *15*, 1860−1864.
(23) Kauzlarich, S. M., Ed. *Chemistry, Structure and Bonding of Zintl Phases and Ions*; VCH Publishers, Inc.: New York, 1996.
(24) Kauzlarich, S. M. Zintl Compounds. In *Encyclopedia of Organic Chemistry*, 2nd ed.; King, R. B., Ed.; John Wiley and Sons: New York, 2005.
(25) Kauzlarich, S. M. *Comments Inorg. Chem.* **1990**, *10* (2−3), 75−88.
(26) Canfield, P. C.; Fisk, Z. *Philos. Mag. B* **1992**, *65* (6), 1117−1123.

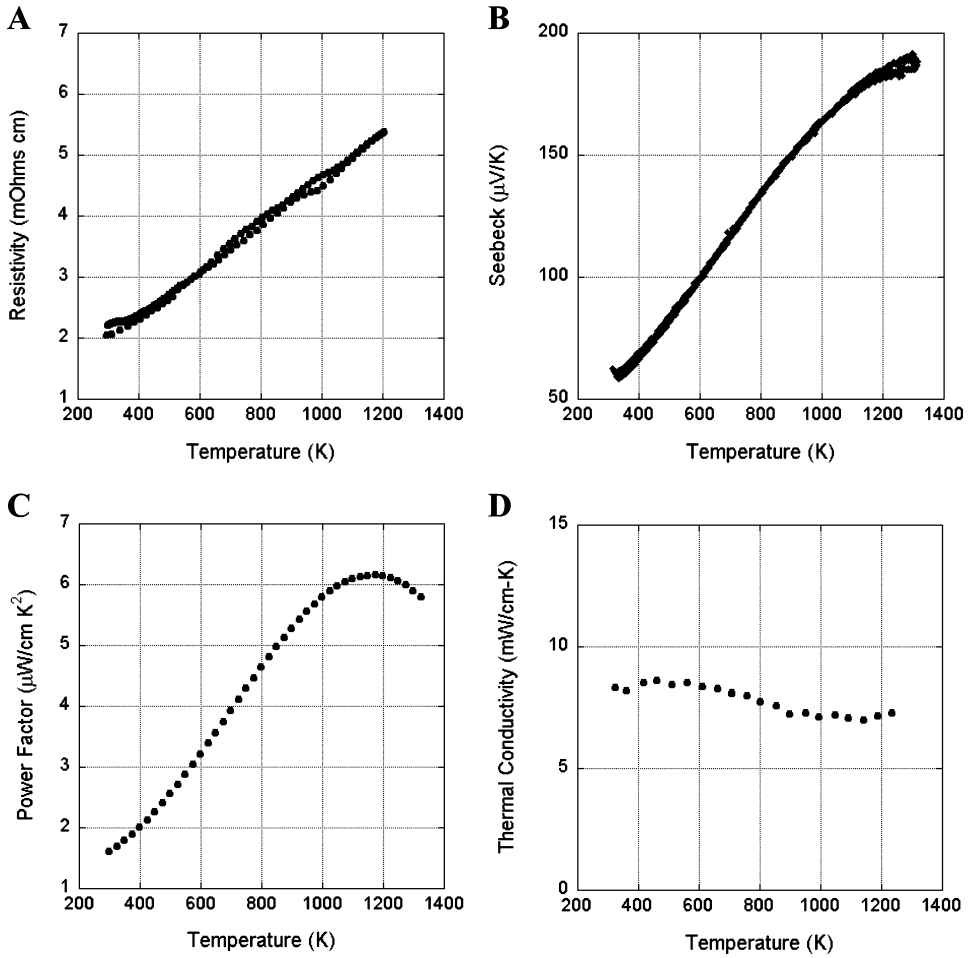


**Figure 2.** (A) Resistivity resulting in a high-temperature value of 5.4 mΩ-cm at 1200 K. Double lines represent heating and cooling scans. (B) Seebeck coefficient reaching a maximum value of +185 $\mu$V/K, indicating p-type behavior. Data presented for both heating and cooling. (C) Power factor ($\alpha^2/\rho$) plot revealing 6 $\mu$W/cm·K$^2$ at 1200 K. (D) Thermal conductivity (mW/cm·K), illustrating a low value of ~7 mW/cm·K at 1150 K.

the reactions were inverted and spun in a centrifuge at 6500 rpm for 3−5 min to separate the products from the Sn flux.

High yields of reflective, silver-colored single-crystal ingots were obtained. All reactions were opened and examined in a nitrogen drybox equipped with a microscope and water levels below 1.0 ppm. Purity was examined using X-ray powder diffraction.

**Thermoelectric Properties Sample Preparation.** To obtain dense samples, finely ground polycrystalline powder was hot-pressed in high-density graphite dies (POCO). A cylinder ~6.5 mm long and 12 mm in diameter was obtained. Experimental density (calculated from measured dimensions and weight) was found to be ~95% of the theoretical density. Hot-pressing was conducted at ~20000 psi and 1223 K for 1.5 h under argon.

For electrical and thermal transport properties, disks (typically 1 mm thick and 12 mm diameter slice) were cut from the cylinder using a diamond saw. Seebeck coefficient measurements were performed on the remaining cylinder. All physical properties were measured between room temperature and 1273 K. Reproducibility of the data was verified with two independently prepared samples.

**Resistivity and Hall Effect.** The electrical resistivity ($\rho$) was measured using the van der Pauw technique with a current of 100 mA and a special high-temperature apparatus.[27] The Hall coefficient was measured in the same apparatus with a forward and reverse magnetic field value of ~10100 G. The carrier density ($n$) was calculated from the Hall coefficient ($R_H$) assuming a scattering factor of 1.0 in a single-carrier scheme, with $n = 1/R_H e$, where $n$ is the densities of charge carriers (holes) and $e$ the charge of the electron. The Hall mobility ($\mu_H$) was calculated from the Hall coefficient and resistivity values with $\mu_H = R_H/\rho$. Data were measured to 1200 K and extrapolated to 1300 K.

**Thermal Conductivity.** The thermal diffusivities were measured for several samples using a flash diffusivity technique.[28] The heat capacity was estimated using the model of Dulong and Petit, $C_p = 3k_B$, for each atom. The thermal conductivity ($\lambda$) was calculated from the calculated heat capacity, experimental density, and experimental thermal diffusivity values. Data were measured to 1223 K and extrapolated to 1300 K.

**Seebeck Coefficient.** The Seebeck coefficient ($\alpha$) was measured using a high-temperature light pulse technique using W/Nb thermocouples.[29]

**Efficiency Calculations.** Exact, optimized, single p-leg efficiencies are calculated according to Snyder.[1] SiGe refers to boron-doped $Si_{0.78}Ge_{0.22}$ used in most recent NASA power sources (GPHS-RTG).

## Results and Discussion

There is no significant change in the electronic or thermal transport properties (Figures 2) of $Yb_{14}MnSb_{11}$ up to 1300 K. These data support the fact that $Yb_{14}MnSb_{11}$ does not

(27) McCormack, J. A.; Fleurial, J. P. *Mater. Res. Soc. Symp. Proc.* **1991**, *234* (Mod. Perspect. Thermoelectr. Relat. Mater.), 135−143.

(28) Vandersande, J. W.; Wood, C.; Zoltan, A.; Whittenberger, D. *Therm. Conduct.* **1988**, *19*, 445−452.

(29) Wood, C.; Zoltan, D.; Stapfer, G. *Rev. Sci. Instrum.* **1985**, *56* (5, Pt. 1), 719−722.

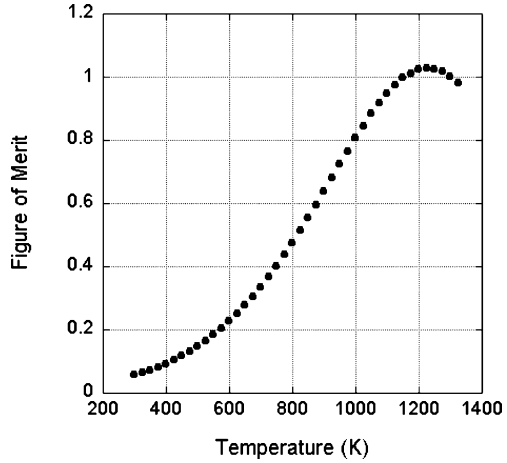


**Figure 3.** Figure of merit of $Yb_{14}MnSb_{11}$. Maximum zT value of ~1.0 at 1200 K.

decompose or change phase within the temperature range needed for deep space power generation.

Hot-pressed pellets of $Yb_{14}MnSb_{11}$ were used to analyze the electronic properties of the material. The resistivity (Figure 2A) linearly increases with increasing temperature and reaches ~5.4 mΩ-cm at 1200 K. The values obtained for the polycrystalline pellets (~2.0 mΩ-cm at 570 K) are slightly larger than that reported for a single crystal (~1.2 mΩ-cm).[14] This is likely due to anisotropy of the resistivity (with higher resistance along the crystallographic *a* axis) rather than grain boundary resistance. The Hall effect provides a constant carrier concentration of $1.1 \pm 0.3 \times 10^{21}$ carriers/cm$^3$ throughout the entire measurement, corresponding to a mobility of about 3 cm$^2$/V·s that decreases with increasing temperature. The Seebeck coefficient (thermopower) for $Yb_{14}MnSb_{11}$ (Figure 2B) reveals a positive increase with increasing temperature and reaches a maximum of +185 $\mu$V/K at 1275 K. The linear resistivity, constant carrier concentration, and linear thermopower are typical of a heavily doped semiconductor. The reduction in the slope of the Seebeck vs temperature curve suggests that the thermopower is about to peak due to thermal activation of minority carriers, indicating an effective band gap of ~0.5 eV.[30] The resulting power factor calculated from the electronic properties reaches a maximum of ~6 $\mu$W/cm·K$^2$ (Figure 2C).

The thermal conductivity of $Yb_{14}MnSb_{11}$ (Figure 2D) was measured using a flash diffusivity technique.[28] The values obtained range between ~7 and 9 mW/cm·K for the temperatures of 300−1275 K (consistent results were observed for several samples). The low value is comparable to a glass,[31,32] heavily contributing to the material's high figure of merit. The low thermal conductivity may be due to the ionically connected components providing a less rigid structure, in a manner similar to $Zn_4Sb_3$, except that for $Yb_{14}MnSb_{11}$, defects appear not to play a role.[32] The low values can also be attributed to the complexity (limiting the phonon mean-free path) and heavy atomic mass (reducing the fraction of atomic vibrational modes that carry heat efficiently) of the crystal.

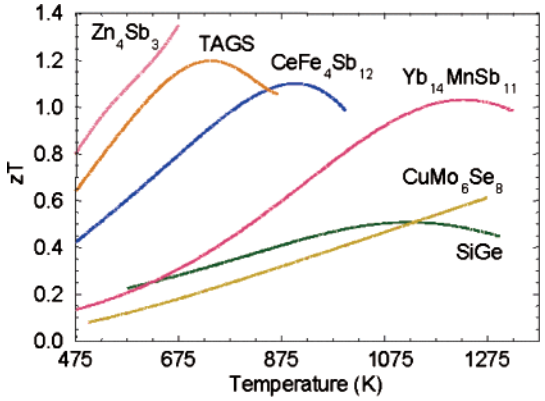


**Figure 4.** Thermoelectric competence of $Yb_{14}MnSb_{11}$ compared to other p-type materials, revealing $Yb_{14}MnSb_{11}$ to be superior over all other materials >975 K (TAGS: $(GeTe)_{0.85}(AgSbTe_2)_{0.15}$).

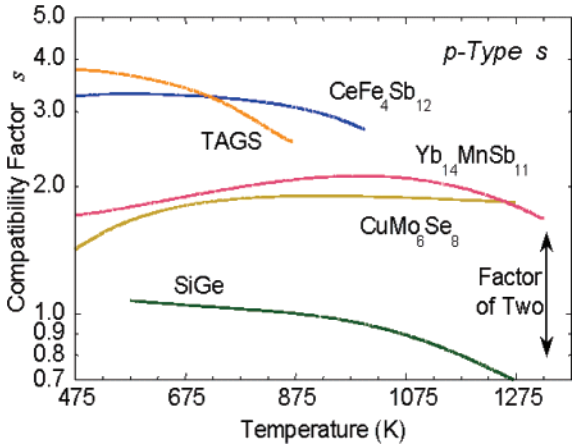


**Figure 5.** Thermoelectric compatibility factor ($V^{-1}$) of $Yb_{14}MnSb_{11}$ compared to other p-type materials. To maintain an optimally operating device, the ratio of compatibility factors between two segmented materials is to remain below a value of 2. The segmentation of $Yb_{14}MnSb_{11}$ with $CeFe_4Sb_{12}$ results in a compatibility factor ratio of <1.5.

As expected, the figure of merit for $Yb_{14}MnSb_{11}$ (Figure 3) sharply increases with increasing temperature and reaches a maximum zT of ~1.0 at 1223 K. Figure 4 compares the most competitive p-type materials, revealing superiority of $Yb_{14}MnSb_{11}$ over the most widely used high-temperature thermoelectric material, SiGe. At elevated temperatures (>900 K) p-SiGe used by NASA reaches a maximum figure of merit of just over 0.5 at 1100 K. Our reported data for $Yb_{14}MnSb_{11}$ has twice the zT of this SiGe.

Applying our results to realistic applications requires segmenting materials in order to create an optimally performing thermoelectric device capable of operating over a large temperature range (300−1275 K). The highest zT materials up to 975 K, $(GeTe)_{0.85}(AgSbTe_2)_{0.15}$ (TAGS) and $CeFe_4Sb_{12}$, have compatibility factors of 3−4 $V^{-1}$ (Figure 5). $Yb_{14}MnSb_{11}$ (2 $V^{-1}$) results in a smaller compatibility difference when compared to SiGe ($s < 1$ $V^{-1}$) and therefore a more efficient system.

In addition, like all thermoelectric materials, for realistic applications, $Yb_{14}MnSb_{11}$ would need to be protected from the environment during operation. This task would not be unachievable seeing as how even SiGe alloys and the

(30) Goldsmid, H. J.; Sharp, J. W. *J. Electron. Mater.* **1999**, *28* (7), 869−872.
(31) Sales, B. C. *Curr. Opin. Solid State Mater. Sci.* **1997**, *2* (3), 284−289.
(32) Snyder, G. J.; Christensen, M.; Nishibori, E.; Caillat, T.; Iversen, B. B. *Nat. Mater.* **2004**, *3* (7), 458−463.

tellurium and antimony rich materials (PbTe, TAGS, skutterudites) react with air and moisture, as well as decompose by sublimation above about 775 K and require encapsulation.

At 975−1275 K, $Yb_{14}MnSb_{11}$ outperforms all reported high-temperature p-type thermoelectric materials, thereby earmarking this system for high-temperature thermoelectric power generation. With a hot side of 1275 K, a cold side of 975 K, and an average zT of 0.95, a 4.3% thermoelectric efficiency is achieved, whereas p-SiGe (average zT of 0.49) achieves only a 2.6% thermoelectric efficiency. Segmenting $Yb_{14}MnSb_{11}$ (1275 to 975 K) with $CeFe_4Sb_{12}$ (975 to 775 K, maximum efficiency 3.4%) increases the efficiency by 3.9% to 7.3%, while that for SiGe/$CeFe_4Sb_{12}$ increases only by 1.1% to 4.5%. As the cold side of the device is lowered to 300 K, the thermoelectric efficiency is enhanced further to a value of 18.6% with the following p-segmentation: $Yb_{14}MnSb_{11}$/$CeFe_4Sb_{12}$/TAGS/$(Bi,Sb)_2Te_3$. Additional improvement of the thermoelectric efficiency should be possible through further doping.

## Conclusion

Bulk $Yb_{14}MnSb_{11}$ has demonstrated unexpected and exceptional thermoelectric properties. It fills the gap where material development was lacking and limiting optimum efficiency of thermoelectric generators. The largest high-temperature figure of merit measured thus far reaches zT ~1.0 (1223 K); for a material that is at the boundary between a Zintl and an intermetallic, this provides a first indication of a potentially rich and exciting field of new thermoelectric compounds. Unlike SiGe, the compatibility factor of $Yb_{14}MnSb_{11}$ is within the acceptable "factor of 2" range required for effective performance of a segmented device, resulting in a quadrupled efficiency improvement. That this progress was achieved with a class of materials that has never had thermoelectric properties (zT) reported is truly a remarkable and significant advance. Additionally, the wide chemical variability of this structure type suggests that this material can be easily optimized and is worthy of further investigations; such ideas are currently under investigation.

**Acknowledgment.** We thank Alexandra Navrotsky for useful discussion. Portions of this work were carried out by the Jet Propulsion Laboratory, California Institute of Technology, under contract with NASA. This research is funded by NASA and NSF.

CM060261T